64 *Chem. Mater.* **2010,** *22,* 64–69
DOI:10.1021/cm902045j

CHEMISTRY OF MATERIALS
Article

CdSe Nanotube Arrays on ITO via Aligned ZnO Nanorods Templating

Minjie Zhou, Haojun Zhu, Xina Wang, Yeming Xu, Yin Tao, Suikong Hark, Xudong Xiao, and Quan Li*

Department of Physics, The Chinese University of Hong Kong, Shatin, New Territory, Hong Kong

Received July 7, 2009. Revised Manuscript Received November 17, 2009

Using a ZnO nanorod array as the template, vertically aligned CdSe nanotubes have been demonstrated on indium tin oxide (ITO) glass in large scale. The wall thickness of the nanotube is tunable and can be increased until the formation of a continuous porous CdSe network. Detailed morphological and structural characterizations of the samples during the nanotube array formation reveal a growth mechanism that can be generally applied to a wide range of materials. In particular, we found that preferable CdSe nucleation and growth on the side surface ($\{10\bar{1}0\}$ planes) of the ZnO nanorods in the array is critical to the later formation of a tubular structure with controllable wall thickness.

Introduction

Since the discovery of carbon nanotubes,[1] inorganic compounds with a tubular structure have attracted great research interest,[2−8] because of the lower density and higher surface-to-volume ratio associated with their specific morphology, extending the capacity for desired surface modification and functionalization. Among various nanotubes, those composed of semiconducting materials take advantage of both the tubular morphology and the unique physical properties of semiconductors, having great potential to serve as functional building blocks for various nanodevice applications, including gas sensing, solar energy conversion, and catalysis.[9] Nevertheless, many device applications would require the assembly of nanotubes into aligned arrays on conducting substrates.[10−14] In this regard, the most reported semiconducting nanotube arrays have been restricted to two material systems, i.e., TiO_2 and ZnO. Although both of them have been utilized as nanostructured electrodes for solar energy conversion devices,[10−14] the application is limited by their large band gaps (> 3 eV); i.e., none of them can simultaneously serve as effective light harvesters.[15] On the other hand, while the formation of ordered TiO_2 nanotube arrays relies on the anodic oxidation of titanium foil,[16] which is a method that is similar to the anodic aluminum oxide (AAO) template fabrication; the tubular array morphology of ZnO is determined by the faster etching rate of its metastable {0001} planes over others in a hexagonal ZnO nanorod.[17] Unfortunately, neither method can be generally applied to the synthesis of nanotube arrays composed of other materials, which could be of interest for different applications.

On the other hand, cadmium selenide (CdSe), with high absorption coefficient and photosensitivity,[18] is one of the most extensively studied Type II−VI semiconductor materials. More importantly, when the size falls in the quantum regime, its band gap can be varied to cover the entire visible spectrum,[19−23] which has great potential for applications in light-emitting devices, solar cell, photodetectors, lasers, and biological labels. Recently, much

*Author to whom correspondence should be addressed. E-mail: liquan@phy.cuhk.edu.hk.

(1) Iijima, S. *Nature* **1991**, *354*, 56.
(2) Tenne, R.; Margulis, L.; Genut, M.; Hodes, G. *Nature* **1992**, *360*, 444.
(3) Chopra, N. G.; Luyken, R. J.; Cherrey, K.; Crespi, V. H.; Cohen, M. L.; Louie, S. G.; Zettl, A. *Science* **1995**, *269*, 966.
(4) Suenaga, K.; Colliex, C.; Demoncy, N.; Loiseau, A.; Pascard, H.; Willaime, F. *Science* **1997**, *278*, 653.
(5) Hacohen, Y. R.; Grunbaum, E.; Tenne, R.; Sloan, J.; Hutchison, J. L. *Nature* **1998**, *395*, 336.
(6) Remskar, M.; Mrzel, A.; Skraba, Z.; Jesih, A.; Ceh, M.; Demšar, J.; Stadelmann, P.; Levy, F.; Mihailovic, D. *Science* **2001**, *292*, 479.
(7) Gautam, U. J.; Vivekchand, S. R. C.; Govindaraj, A.; Kulkarni, G. U.; Selvi, N. S.; Rao, C. N. R. *J. Am. Chem. Soc.* **2005**, *127*, 3658.
(8) Xu, F. F.; Hu, J.; Bando, Y. *J. Am. Chem. Soc.* **2005**, *127*, 16860.
(9) Rao, C. N. R.; Govindaraj, A. *Nanotubes and Nanowires*; RSC Publishing: Cambridge, U.K., 2005.
(10) Mor, G. K.; Shankar, K.; Paulose, M.; Varghese, O. K.; Grimes, C. A. *Nano Lett.* **2005**, *5*, 191.
(11) Mor, G. K.; Shankar, K.; Paulose, M.; Varghese, O. K.; Grimes, C. A. *Nano Lett.* **2006**, *6*, 215.
(12) Zhu, K.; Neale, N. R.; Miedaner, A.; Frank, A. J. *Nano Lett.* **2007**, *7*, 69.
(13) Martinson, A. B. F.; Elam, J. W.; Hupp, J. T.; Pellin, M. J. *Nano Lett.* **2007**, *7*, 2183.
(14) Shankar, K.; Bandara, J.; Paulose, M.; Wietasch, H.; Varghese, O. K.; Mor, G. K.; LaTempa, T. J.; Thelakkat, M.; Grimes, C. A. *Nano Lett.* **2008**, *8*, 1654.
(15) Shockley, W.; Queisser, H. J. *J. Appl. Phys.* **1961**, *32*, 510.
(16) Mor, G. K.; Varghese, O. K.; Paulose, M.; Shankar, K.; Grimes, C. A. *Sol. Energy Mater. Sol. Cells* **2006**, *90*, 2011.
(17) Vayssieres, L.; Keis, K.; Hagfeldt, A.; Lindquist, S. E. *Chem. Mater.* **2001**, *13*, 4395.
(18) Jager-Waldau, R.; Stucheli, N.; Braun, M.; Lux-Steiner, M.; Bucher, E.; Tenne, R.; Flaisher, H.; Kerfin, W.; Braun, R.; Koschel, W. *J. Appl. Phys.* **1988**, *64*, 2601.
(19) Murray, C. B.; Norris, D. J.; Bawendi, M. G. *J. Am. Chem. Soc.* **1993**, *115*, 8706.
(20) Murray, C. B.; Kagan, C. R.; Bawendi, M. G. *Science* **1995**, *270*, 1335.
(21) Kagan, C. R.; Murray, C. B.; Nirmal, M.; Bawendi, M. G. *Phys. Rev. Lett.* **1996**, *76*, 1517.
(22) Bruchez, M.; Moronne, M.; Gin, P.; Weiss, S.; Alivisatos, A. P. *Science* **1998**, *281*, 2013.
(23) Peng, J. A.; Peng, X. *J. Am. Chem. Soc.* **2001**, *123*, 183.

 Published on Web 12/04/2009 © 2009 American Chemical Society

research effort has also been devoted to the fabrication of various CdSe-based nanostructures,[24−31] which may find applications in future nanodevices. In particular, CdSe nanotube is of special interest, because of the increased active surface area, compared to its other one-dimensional morphologies. Indeed, CdSe nanotubes have been fabricated using a sonoelectrochemical technique[32] and templating methods, when selenium nanowires,[33] tin nanowires,[34] cadmium nanowires,[35] $Cd(OH)_2$ nanowires,[36] and AAO[37] have been employed as the template materials. Nevertheless, large-scale synthesis of the nanotubes into an aligned array configuration and on conducting substrates remains challenging.

In the present work, we demonstrate a synthetic route for aligned nanotube arrays formation on conducting substrates by taking the CdSe nanotube array-on-ITO structure as an example. We show that the walls of these CdSe nanotubes can be controlled at different thicknesses, and, in the extreme case, a continuous nanoporous CdSe network is obtained. Detailed characterizations on the sample morphologies, compositions, and photoluminescence (PL) properties have been performed during the nanotube formation process, based on its growth mechanism, are discussed in detail.

Results and Discussions

Morphology, Structure, and Chemical Composition of the Samples during the CdSe Nanotube Array Formation. The formation process of the CdSe nanotube arrays is illustrated by scanning electron microscopy (SEM) images taken at different synthetic steps (see Figure 1). The ZnO nanorod array-on-ITO structure has been used as the starting template (Figure 1a). The individual ZnO nanorod has a hexagonal cross section, low-indexed termination surfaces ({0002} planes as the top surface, and $\{10\bar{1}0\}$ planes as the side surfaces), which appear to be smooth (see the inset of Figure 1a). The diameter of the ZnO nanorods is 400 ± 50 nm in this sample series. After CdSe deposition, the surface of these ZnO nanorods becomes rough with its diameter increasing to 800 ± 60 nm, although the aligned array configuration remains intact (see Figure 1b). The etching of ZnO in the ammonia solution results in distinct nanotubes arrays, and further annealing of such a sample (in air) causes little morphological change (see Figure 1c). The inner and outer diameters of the nanotubes are estimated to be ~400 ± 50 nm and ~800 ± 60 nm, which is consistent with that of the original ZnO nanorod and the ZnO-core/CdSe-shell nanocables in the arrays, respectively. Figure 1d shows a side view of the CdSe nanotube arrays, obtained by clipping the sample off the substrate. The length of the nanotubes in the array is determined by the length of the original ZnO nanorods template, and it can be controlled in a size range from several hundreds of nanometers to > 10 μm.

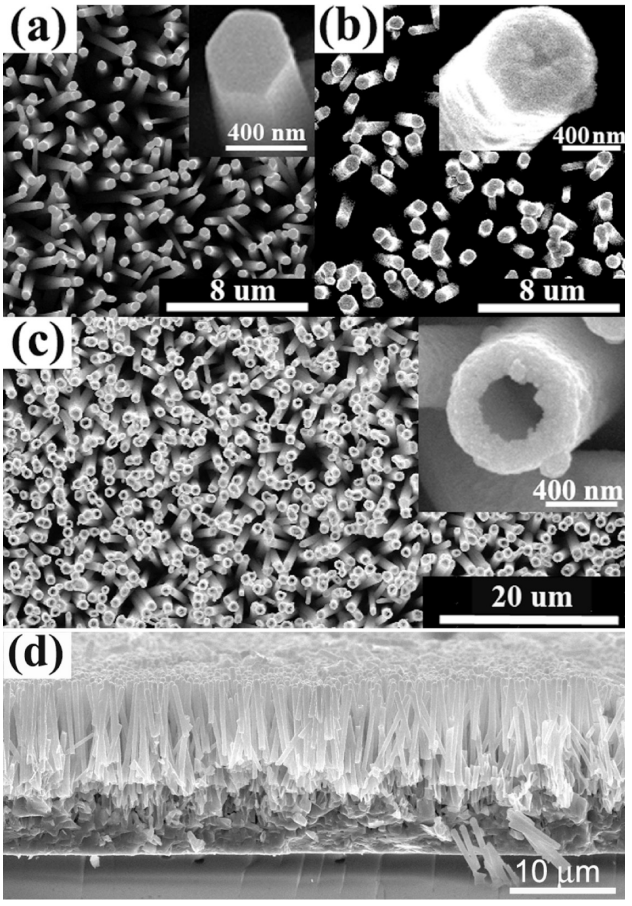

Figure 1. Scanning electron microscopy (SEM) images of (a) the ZnO nanorod, (b) the ZnO/CdSe nanocable, and (c) the annealed CdSe nanotube. (Insets in the upper right corner of each panel show a high-magnification image of each.)

The crystallinity of the above samples has been studied by X-ray diffraction (XRD), at which point their structural evolution is revealed (see Figure S1 in the Supporting Information). Although diffraction peaks of CdSe appear after the electrochemical deposition of CdSe on ZnO, they are very broad, which suggests the poor crystallinity and/or small grain size of the CdSe shell on ZnO nanorods in the array. As a comparison, air annealing of the nanotube sample results in much sharper diffraction peaks, which can be indexed to hexagonal CdSe. No impurity peak has been detected, excluding possible sample oxidation during the annealing process.

(24) Chen, C. C.; Chao, C. Y.; Lang, Z. H. *Chem. Mater.* **2000**, *12*, 1516.
(25) Peng, Z. A.; Peng, X. *J. Am. Chem. Soc.* **2002**, *124*, 3343.
(26) Tang, K.; Qian, Y.; Zeng, J.; Yang, X. *Adv. Mater.* **2003**, *15*, 448.
(27) Shan, C. X.; Liu, Z.; Hark, S. K. *Appl. Phys. Lett.* **2005**, *87*, 163108.
(28) Kanaras, A. G.; Sonnichsen, C.; Liu, H.; Alivisatos, A. P. *Nano Lett.* **2005**, *5*, 2164.
(29) Wang, Z. Y.; Fang, X. S.; Lu, Q. F.; Ye, C. H.; Zhang, L. D. *Appl. Phys. Lett.* **2006**, *88*, 083102.
(30) Li, L.; Hu, J.; Yang, W.; Alivisatos, A. P. *Nano Lett.* **2007**, *1*, 349.
(31) Cheng, J. H.; Chao, H. Y.; Chang, Y. H.; Hsu, C. H.; Cheng, C. L.; Chen, T. T.; Chen, Y. F.; Chu, M. W. *Physica E* **2008**, *40*, 2000.
(32) Shen, Q. M.; Jiang, L. P.; Miao, J. J.; Hou, W. H.; Zhu, J. J. *Chem. Commun.* **2008**, *112*, 1683.
(33) Jiang, X. C.; Mayers, B.; Herricks, T.; Xia, Y. *Adv. Mater.* **2003**, *15*, 1740.
(34) Hu, J. Q.; Bando, Y.; Zhan, J. H.; Liao, M. Y.; Golberg, D.; Yuan, X. L.; Sekiguchi, T. *Appl. Phys. Lett.* **2005**, *87*, 113107.
(35) Rao, C. N. R.; Raidongia, K. *J. Phys. Chem. C* **2008**, *112*, 13366.
(36) Shim, H. S.; Shinde, V. R.; Kim, J. W.; Gujar, T. P.; Joo, O. S.; Kim, H. J.; Kim, W. B. *Chem. Mater.* **2009**, *21*, 1875.
(37) Lin, T. J.; Chen, C. C.; Cheng, S.; Chen, Y. F. *Opt. Express* **2008**, *16*, 671.

A more-detailed structure/chemical composition change during the nanotube formation can be clearly observed in the transmission electron microscopy (TEM)-related study of the corresponding samples (see Figure 2). ZnO nanorods with a smooth surface are found in the original ZnO nanorod array template sample (see Figure 2a). Selected-area diffraction (SAD), taken from a single nanorod, reveals its signal crystalline nature (taken from the ZnO [$2\bar{1}\bar{1}0$] zone axis), while the corresponding energy-dispersive X-ray (EDX) spectrum only shows signals from Zn and O, with the Zn:O ratio close to 1 (see Figure 2a; the Cu signal in all of the EDX spectra comes from the TEM supporting grid). The surface of the ZnO nanorod becomes rough after CdSe deposition (see Figure 2b). Other than the diffraction spots from ZnO, diffused ring patterns that can be indexed to the hexagonal CdSe also appear in the SAD taken from such a sample. Consistently, signals from Cd and Se appear together with Zn and O in the EDX spectrum, with both the Cd:Se and the Zn:O ratios being close to 1 (see Figure 2b). Removal of the ZnO nanorod core leads to a hollow nanotube configuration (see Figure 2c), which is mainly composed of Cd and Se (Cd:Se ratio ≈ 1). In the SAD pattern of such a nanotube, only a diffused ring pattern exists and can be indexed to the hexagonal CdSe, indicating the polycrystalline nature of the as-synthesized nanotubes (see Figure 2c). Air annealing of the CdSe nanotubes does not cause any morphological or chemical compositional changes to them, as revealed, respectively, by the low-magnification TEM image and EDX spectrum shown in Figure 2d. Nevertheless, the diffraction rings in the SAD of the annealed nanotube become shaper, suggesting improved crystallinity and/or increased grain size of CdSe in the tube. This is consistent with the high-resolution electron microscopy (HREM) images taken from the as-synthesized (Figure 2e) and annealed (Figure 2f) nanotube samples; one can estimate that the size of the nanocrystals in the polycrystalline CdSe nanotube increases from 10 ± 5 nm in the as-synthesized sample to ≥ 20 nm in the annealed ones. The small grain size in the as-synthesized sample makes it difficult to tilt individual crystals to a proper zone axis, so that analysis of the lattice fringes would not generate any accurate information. Figure 2f is a HREM image taken from the [0001] zone axis, the *d*-spacing of the lattice fringes are measured as 0.37 nm, matching those of {$10\bar{1}0$} planes of hexagonal CdSe.

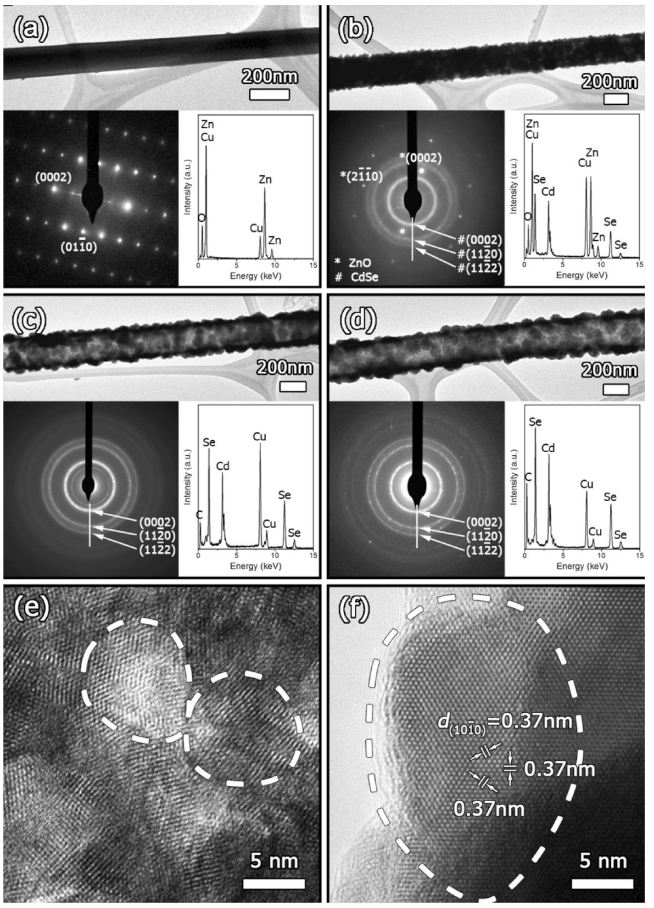

Figure 2. Low-magnification TEM images and the corresponding selected-area diffraction (SAD) patterns and EDX spectra of (a) the ZnO nanorod, (b) the ZnO/CdSe core/shell nanocable, (c) the as-grown CdSe nanotube, and (d) the annealed CdSe nanotube. Panels (e) and (f) show HREM images of as-grown and annealed CdSe nanotubes, respectively.

Tunable Diameter and Wall Thickness of the CdSe Nanotubes. The diameter of the CdSe nanotube is tunable and primarily determined by the size of the ZnO nanorod in the original array template. Figure 3 show the SEM images of three CdSe nanotube samples formed using ZnO nanorods with diameters of $\sim 50 \pm 10$, $\sim 150 \pm 25$, and $\sim 400 \pm 50$ nm as the original template, and one can see that the resulted CdSe nanotube samples have diameters of $\sim 50 \pm 10$, $\sim 150 \pm 25$, and $\sim 400 \pm 50$ nm, accordingly.

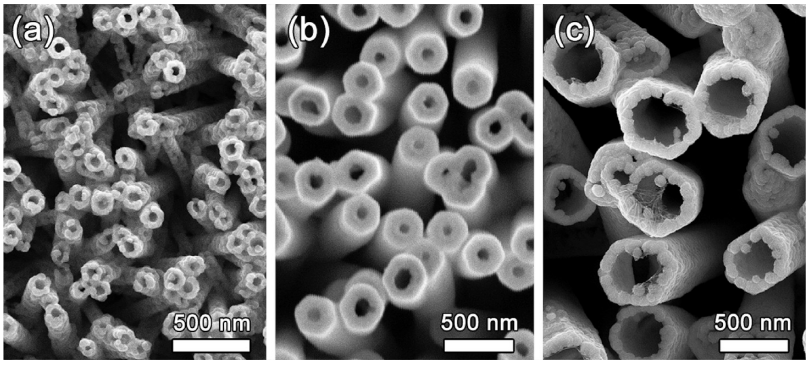

Figure 3. SEM images of CdSe nanotube arrays with variable inner diameters of (a) ~50, (b) ~150, and (c) ~400 nm.

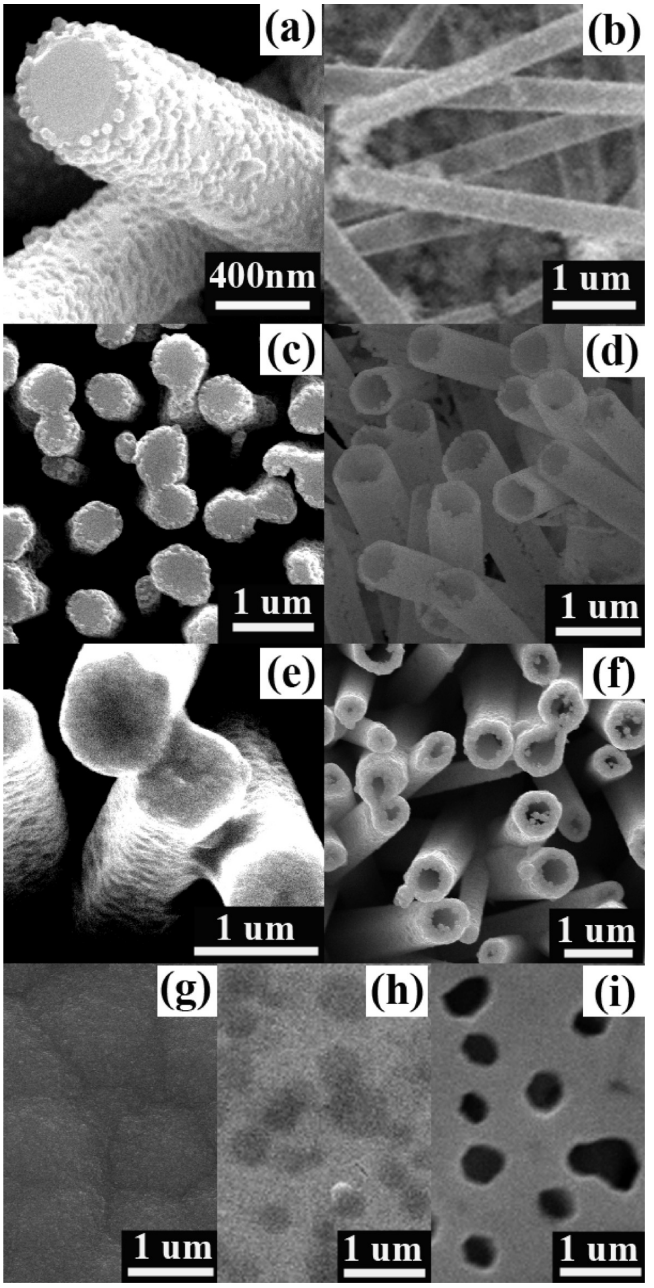

Figure 4. SEM images of ZnO/CdSe composite nanostructures and the resulting CdSe hollow nanostructures, with (a, b) 5 min, (c, d) 10 min, (e, f) 20 min, and (g, h, i) 120 min of CdSe deposition. Panel (h) shows the sample given in panel (g) after mechanical polishing.

The thickness of the CdSe shell can be controlled by adjusting the electrochemical deposition time. This allows a tunable wall thickness to be achieved in the CdSe nanotubes. In fact, we have identified a distinct morphology evolution of the CdSe nanotubes at a later stage when the CdSe shell thickness is controlled at different levels during the electrochemical deposition. The short deposition duration ($\leq$5 min) leads to a very thin layer of CdSe (in the form of particle aggregates) on ZnO, and, in the extreme case, full coverage of the ZnO nanorod surface may not be achieved (see Figure 4a). The removal of ZnO in such a sample would completely destroy the aligned array configuration on ITO, although collapsed CdSe nanotubes randomly scattered on the substrate can be

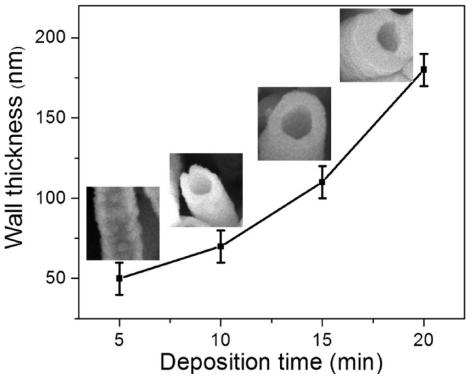

Figure 5. Change in CdSe wall thickness, as a function of the electrochemical deposition time.

observed in some regions of the sample (see Figure 4b). A longer deposition time definitely results in a thicker CdSe shell on ZnO (see Figures 4c (10 min deposition) and 4e (20 min deposition)) and, consequently, a more robust nanotube array on ITO after ZnO etching (see Figures 4d and 4f). Figure 5 plots the change in the CdSe wall thickness as a function of the electrochemical deposition time. The wall thicknesses of the CdSe nanotube are ~50, ~70, ~110, and ~180 nm (with a standard deviation of 10 nm) when deposited for 5, 10, 15 and 20 min, respectively. Note that a further increase in CdSe deposition time would eventually lead to the disappearance of the nanocable array morphology, because of the formation of a continuous ZnO-nanorod/CdSe-matrix composite film on the ITO substrate (see Figure 4g, 120 min deposition). By removing the top surface CdSe layer in such a composite film using mechanical polishing, the morphology of continuous ZnO-nanorod/CdSe-matrix can be clearly observed (see Figure 4h). Further ZnO etching in such a sample results in a continuous network of porous CdSe (see Figure 4i).

Formation Mechanism of the CdSe Nanotube Arrays on ITO. Now, we discuss the formation mechanism of the CdSe nanotube arrays on an ITO substrate. The growth pattern of the CdSe on ZnO during the electrochemical deposition is critical to the tubular morphology formed at a later stage. The large surface area of the ZnO nanorods serves as preferable nucleation sites for the incoming Cd and Se species in the solution. Comparing the two types of termination surface of the ZnO nanorods, i.e., side surface consisted of $\{10\bar{1}0\}$ planes and top surface of {0002} planes (inset of Figure 1a), preferable nucleation and growth of CdSe first occurs at the side surface, resulting in a faster wrapup of the ZnO nanorod on the side walls (see Figures 4a, 4c, and 4e) and leaving the top openings as channels for later ZnO etching. Such a growth pattern also allows faster CdSe shell expansion along the nanocable radial direction while maintaining the aligned array configuration until the empty space among the ZnO nanorods is fully filled; a continuously CdSe matrix formation, then followed by complete top surface coverage by CdSe, also occurs (see Figure 4g).

Two synthesis parameters are found to be crucial in achieving the nanotube morphology of CdSe. The

first one is the choice of the etching solutions for ZnO. In principle, ZnO can be etched under both acidic and alkaline solutions, i.e., $ZnO + 2H^+ = Zn^{2+} + H_2O$ and$ZnO + 2OH^- = ZnO_2^{2-} + H_2O$Nevertheless, the reaction between ZnO and most acids is intense and difficult to control. In addition, the deposited CdSe would also dissolve in an acidic environment. On the other hand, etching of ZnO in an alkaline solution is observed to be slow; little morphology change is observed after the sample is soaked into an alkaline solution (e.g., NaOH) at pH ~13 for 10 h. Although ammonia is a weak alkali, it reacts with ZnO via the formation of a zinc tetraamine complex: $ZnO + 4NH_3 \cdot H_2O = Zn(NH_3)_4^{2-} + 2OH^- + 3H_2O$ Such a reaction can effectively "dissolve" the ZnO while, at the same time, being mild enough to maintain the nanotube array morphology of CdSe. The second parameter is the structural quality of the CdSe in the ZnO/CdSe core/shell nanocables. Although the top surface (either uncovered or partially covered ZnO {0002} planes) serves as the primary route for the etchant solution to flow in, solution permeation through the CdSe side walls also makes a important contribution. In this regard, the defective and loose structure of CdSe with poor crystallinity that resulted from the electrochemical deposition is determined to be beneficial, because it provides easy permeation channels for the etching chemicals. Indeed, when the nanocable sample is annealed (in air) before etching, one would find improved crystallinity of CdSe but, at the same time, ineffective removal of the ZnO core (see Figure S2 in the Supporting Information).

Absorption and Photoluminescence (PL) Properties. The evolution in the photoluminescence (PL) of the samples is consistent with the nanotube array formation process. The strong near-band-edge emission (NBE) of ZnO in the nanorod array template is found to be significantly depressed (see Figure 6a) when CdSe is deposited on its surface. A similar trend (Figure 6b) is observed for CdSe, i.e., while the NBE of CdSe in the nanocables is extremely low, removal of the ZnO nanorod cores leads to a huge surge of such emissions. Annealing of the CdSe nanotubes further enhances its NBE, mainly because of the removal of various defects centers. The drastic decrease in the NBE intensities of both ZnO and CdSe (in the nanocables) originates from the Type II band alignment between ZnO and CdSe, which reduces residual electron−hole overlapping and, thus, their recombination probability in the individual materials.[38−40]

The PL emission of the CdSe nanotubes should originate from the material's band-edge emissions. A blue shift in the emission energy has been observed in the as-synthesized CdSe nanotube, compared to the annealed ones, suggesting possible grain size enlargement in the annealed samples. This is consistent with the TEM observation of the sample-grain growth is obvious in the corresponding HREM images. Estimation of the band gaps of the as-synthesized and annealed CdSe nanotube

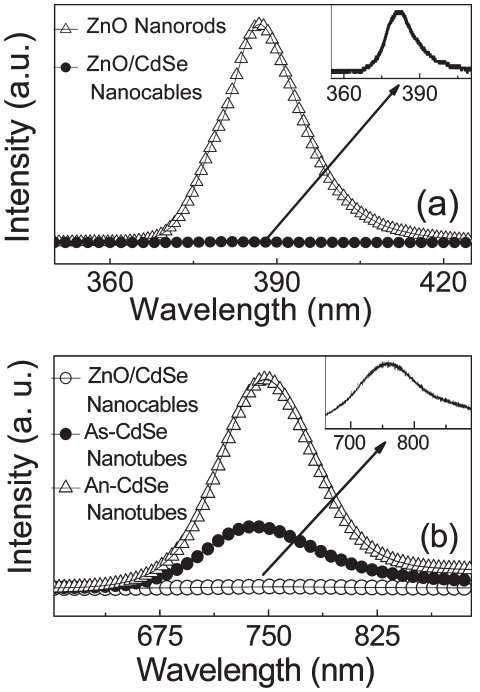

Figure 6. Room-temperature photoluminescence (PL) spectra: (a) ZnO near-band-edge emission (NBE) in ZnO nanorods and ZnO/CdSe nanocables; and (b) CdSe NBE in ZnO/CdSe nanocables, as-prepared (denoted by the prefix As-), and annealed (denoted by the prefix An-) CdSe nanotubes.

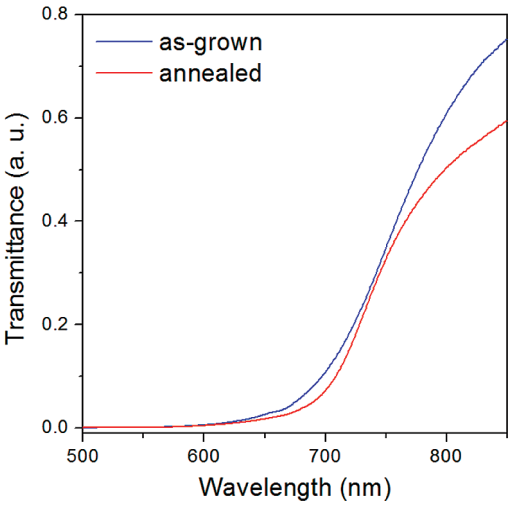

Figure 7. Absorption spectra of as-grown (blue trace) and annealed (red trace) CdSe nanotube arrays on an ITO substrate.

samples has been made from the absorption spectra taken from the two samples (see Figure 7). The optical absorption near the band edge can be described by$\alpha = \frac{A(h\nu - E_g)^n}{h\nu}$ where α is the absorption coefficient, A a constant, $h\nu$ the incident photon energy, E_g and the optical band gap energy; the value of n is dependent on whether the transition is direct ($n = {}^1/_2$) or indirect ($n = 2$).[41] By plotting $(\alpha h\nu)^{1/n}$ as a function of $h\nu$ ($n = {}^1/_2$ in the present case), one can extrapolate the value of E_g. While the band gap of the anneal nanotube is ~1.74 eV, being consistent with the literature value of bulk CdSe, that of the

(38) Swank, R. K. *Phys. Rev.* **1967**, *153*, 844.
(39) Zhang, Y.; Wang, L. W.; Mascarenhas, A. *Nano Lett.* **2007**, *7*, 1264.
(40) Kumar, S.; Jones, M.; Lo, S.; Scholes, G. *Small* **2007**, *3*, 1633.
(41) Butler, M. A. *J. Appl. Phys.* **1977**, *48*, 1914.

as-synthesized ones is slightly higher (i.e., ~1.77 eV). The blue shift of the band gap in the as-synthesized samples is likely induced by the quantum confinement effect, because small-sized CdSe crystals exist in such a sample (≤10 nm in diameter, as observed in the HREM images), the value of which is close to the Bohr radius of CdSe (~5 nm).

Conclusions

In conclusion, large-scale CdSe nanotube arrays on ITO have been demonstrated using a simple ZnO nanorod templating-etching method. The preferred nucleation and growth of CdSe on the side surface of ZnO nanorods in the array determines the later formation of tubular array morphology with controllable tube wall thickness that can be increased until continuous CdSe porous network formation. The present methodology can be generally applied to a wide range of materials. Using ZnO nanostructures with different morphologies (such as nanobelt, tetrapod, etc.), versatile hollow structures of different materials are expected, via such a synthetic route, providing diversified building blocks that may be required for various nanodevice applications.

Methods

The ZnO nanorod array-on-ITO[42] format has been used as the template for the CdSe nanotube formation. The CdSe was first deposited on the surface of the ZnO nanorods in the array using electrochemical deposition.[43] In a typical procedure, an aqueous solution of 0.05 M cadmium acetate, 0.1 M nitrilotriacetic acid trisodium salt, and 0.05 M selenosulfate (with excess sulfite) were used. The CdSe was deposited galvanostatically (at a current density of ~2.7 mA/cm^2) at room temperature in a two-electrode electrochemical cell, with the ZnO nanorod array-on-ITO structure as the cathode and platinum metal as the counterelectrode. The CdSe deposition time is 20 min, unless specified. After CdSe deposition, the entire sample (on ITO) was dipped into a 25% ammonia solution for 1 h to remove the ZnO nanorods, which is a process that leads to the formation of CdSe nanotube arrays on ITO. Finally, the nanotube sample was annealed at 350 °C in air for 1 h.

The general morphology and crystallinity of the samples were examined by scanning electron microscopy (SEM; Quantum Model F400), and X-ray diffraction (XRD; Rigaku Model RU300), respectively. Their microstructure and chemical composition were investigated by transmission electron microscopy (TEM; Tecnai Model 20 FEG), with an energy-dispersive X-ray (EDX) spectrometer attached to the same microscope. The TEM samples were prepared by removing the nanotubes from the substrate, dispersing them into alcohol, and then depositing them onto a lacey-carbon-film TEM grid. The absorption of the samples were examined using a Hitachi Model U3501 UV−vis absorption spectrometer. Near-band-edge emission (NBE) of both ZnO and CdSe are studied by room-temperature photoluminescence (PL) measurements, using the 325-nm line of a HeCd laser for ZnO, and the 514-nm line of an argon laser for CdSe.

Acknowledgment. This work is supported by grants from the GRF of HKSAR (under Project No. 414908, CUHK Focused Investment Scheme C, and CUHK Group Research Scheme).

Supporting Information Available: XRD spectra of the ZnO nanorod, the ZnO/CdSe nanocable, and the annealed CdSe nanotube (Figure S1), and an SEM photomicrograph of the air-annealed ZnO/CdSe nanocable sample after being etched in ammonia for 1 hr (Figure S2). (PDF) This material is available free of charge via the Internet at http://pubs.acs.org.

(42) Zhou, M. J.; Zhu, H. J.; Jiao, Y.; Rao, Y. Y.; Hark, S. K.; Liu, Y.; Peng, L. M.; Li, Q. *J. Phys. Chem. C* **2009**, *113*, 8945.
(43) Tena-Zaera, R.; Ryan, M. A.; Katty, A.; Hodes, G.; Bastide, S.; Levy-Clement, C. *C. R. Chim.* **2006**, *9*, 717.